AD-A099 828 ARMY ELECTRONICS RESEARCH AND DEVELOPMENT COMMAND FO--ETC F/G 20/12
PROXIMITY EFFECTS IN ELECTRON BEAM LITHOGRAPHY.(U)
APR 81 G J IAFRATE, C F COOK, J KWIATKOWSKI
UNCLASSIFIED DELET-TR-81-11 NL

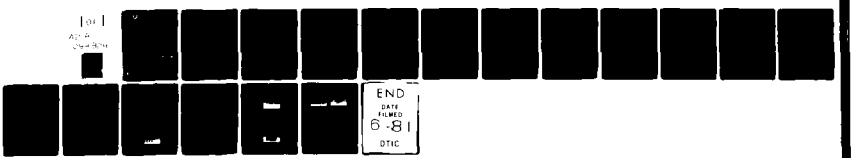

END
DATE FILMED
6-81
DTIC

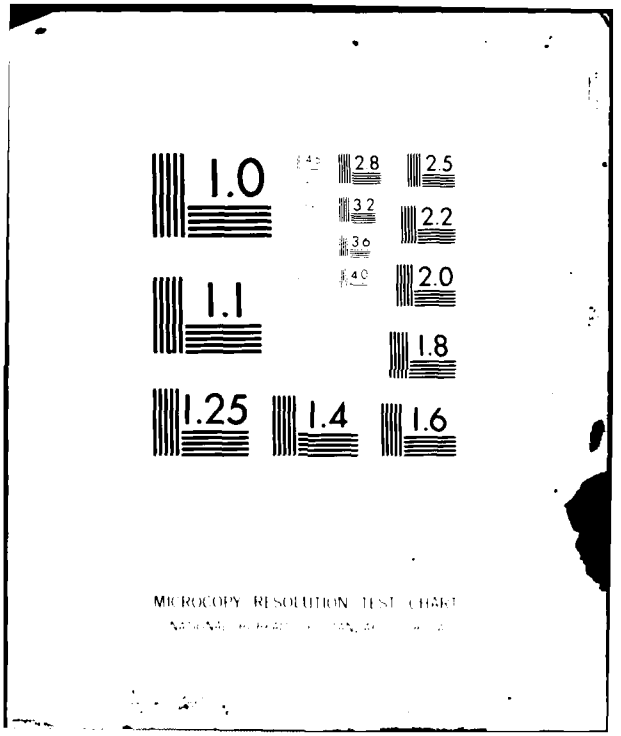
1.0
2.8
2.5
3.2
2.2
3.6
4.0
2.0
1.1
1.8
1.25
1.4
1.6
MICROCOPY RESOLUTION TEST CHART

LEVEL

(12)

RESEARCH AND DEVELOPMENT TECHNICAL REPORT

DELET-TR-81-11

PROXIMITY EFFECTS IN ELECTRON BEAM LITHOGRAPHY

G. J. IAFRATE
C. F. COOK, JR.
J. KWIATKOWSKI

ELECTRONICS TECHNOLOGY & DEVICES LABORATORY

APRIL 1981

ERADCOM

US ARMY ELECTRONICS RESEARCH & DEVELOPMENT COMMAND
FORT MONMOUTH, NEW JERSEY 07703

NOTICES

Disclaimers

The citation of trade names and names of manufacturers in this report is not to be construed as official Government indorsement or approval of commercial products or services referenced herein.

Disposition

Destroy this report when it is no longer needed. Do not return it to the originator.

UNCLASSIFIED

SECURITY CLASSIFICATION OF THIS PAGE (When Data Entered)

REPORT DOCUMENTATION PAGE		READ INSTRUCTIONS BEFORE COMPLETING FORM
1. REPORT NUMBER (14) DELET-TR-81-11	2. GOVT ACCESSION NO. AD-A099	3. RECIPIENT'S CATALOG NUMBER 828
4. TITLE (and Subtitle) (6) PROXIMITY EFFECTS IN ELECTRON BEAM LITHOGRAPHY.		5. TYPE OF REPORT & PERIOD COVERED
		6. PERFORMING ORG. REPORT NUMBER
7. AUTHOR(s) (10) G.J. Iafrate, C.F. Cook, Jr., J. Kwiatkowski		8. CONTRACT OR GRANT NUMBER(s) (15) 121
9. PERFORMING ORGANIZATION NAME AND ADDRESS Electronic Materials Research Division US Army Electronics Technology & Devices Lab Fort Monmouth, NJ 07703 DELET-ED		10. PROGRAM ELEMENT, PROJECT, TASK AREA & WORK UNIT NUMBERS 611102A (17) (16) 1L161102AH47,01,011
11. CONTROLLING OFFICE NAME AND ADDRESS (11) USA Electronics Research & Development Command Fort Monmouth, NJ 07703 DELET-ED		12. REPORT DATE Apr[illegible]981 13. NUMBER OF PAGES 12
14. MONITORING AGENCY NAME & ADDRESS (if different from Controlling Office) (9) Technical Repts.		15. SECURITY CLASS. (of this report) UNCLASSIFIED 15a. DECLASSIFICATION/DOWNGRADING SCHEDULE

16. DISTRIBUTION STATEMENT (of this Report)

Approved for public release; distribution unlimited.

17. DISTRIBUTION STATEMENT (of the abstract entered in Block 20, if different from Report)

18. SUPPLEMENTARY NOTES

19. KEY WORDS (Continue on reverse side if necessary and identify by block number)

Electron Beam Lithography, Proximity Effects, Electron Scattering in Resists

20. ABSTRACT (Continue on reverse side if necessary and identify by block number) The required miniaturization of military IC devices to submicron and ultra-submicron dimensions in the 1980s raises serious questions regarding the use of electron beam (e-beam) lithography as an appropriate fabrication technique for this end. In this paper it is shown that the ultimate resolution of the e-beam process is determined by electron scattering effects in the lithographic resist material and by electron back-scattering from the underlying device substrate. The merit of the e-beam fabrication technique for use in very high speed integrated circuit (VHSIC) technology
(cont'd on reverse side)

DD FORM 1 JAN 73 1473 EDITION OF 1 NOV 65 IS OBSOLETE

UNCLASSIFIED

SECURITY CLASSIFICATION OF THIS PAGE (When Data Entered)

is assessed. A study is presented which describes the electron scattering and backscattering processes in electronic materials. A theoretical analysis describing primary electron backscattering from single- and double-layered substrates is presented; also, attention is focused on the question of the spatial region exposed by a scattered e-beam in a lithographic e-beam resist material. Experimental electron backscattering, e-beam, and scanning electron microscopy studies are used to corroborate theoretical findings.

CONTENTS

	Page
INTRODUCTION	1
ELECTRON BACKSCATTERING	2
ELECTRON SCATTERING	7
ELECTRON-BEAM LITHOGRAPHIC STUDIES	9
SUMMARY	12
ACKNOWLEDGMENTS	12

FIGURES

1. Electron backscatter coefficients for B, Si, Ti & Ge for various retarding voltages. 3

2. Energy distribution curves for electrons backscattered from B, Si, Ti & Ge. 3

3. Comparison of EDC's of Everhart's theory with those experiments obtained in ref. (6) for Al, Cu, and Pt. 4

4. Backscattering coefficient for double layer targets. Z_1 and Z_2 refer to the average nuclear charge of the thin film and substrates, respectively; y_D is the reduced thin film thickness. 5

5. EDC's for double-layer targets. Z_1 and Z_2 refer to the average nuclear charge of the thin film and substrates, respectively; Y_D is the reduced thin film thickness. 5

6. Comparison of η for multilayer films of aluminum over gold and aluminum over carbon. 6

7. Comparison of η_{TF} with experiment for Cu. 6

8. Plot of $\langle\cos\theta\rangle$ as a function of normalized depth, y_D, with average atomic number, Z, as a parameter. 7

9. Diagram depicts two e-beams, separated by a distance D, striking the target; the geometrical angle, θ_g, and the undercutting length, L, are visually defined. 8

10. Plot of reduced depth, L, as a function of reduced separation, D, with average atomic number, Z, as a parameter. 8

Page

11. SEM photograph of a typical EBL exposure of thick PMMA resist material. 9

12. SEM photograph of e-beam radiation pattern. 11

13a. SEM photograph of e-beam exposure on PMMA. 11

13b. SEM photograph of e-beam exposure on PMMA/silicon substrate. 12

13c. SEM photograph of e-beam exposure on PMMA/gold substrate. 12

INTRODUCTION

Future military requirements for real-time information acquisition and tactical electronic warfare (EW) information processing have established a need for very large scale (VLS) and very high speed (VHS) integrated circuit microelectronics. Both VLSI and VHSI technologies require a high areal density of integrated circuit (IC) elements thereby dictating a reduction of device size into the submicron and ultra-submicron regions.

The requisite miniaturization of military IC devices into the submicron and ultra-submicron region raises serious questions regarding the use of electron beam lithography (EBL) as an appropriate fabrication technique for this end. In EBL an intermediate energy (5-20 keV) electron beam exposes a radiation sensitive target (such as the polymer PMMA) overlaid on an IC device substrate; a subsequent chemical development treatment removes the exposed region leaving an outline of the pattern sketched by the electron beam (e-beam) when employing a positive-acting resist. The e-beam technique is attractive because it leads to the production of micron to submicron resolved channels and also lends itself to computer-controlled production-line automation. However, we find that the use of an e-beam introduces certain difficulties in that electrons penetrating the target scatter away from the incident electron beam thereby causing unintended exposure to other regions of the target; also, the penetrating electrons are generally energetic enough to reach and backscatter from the IC substrate thus tending to expose unintended regions of the resist as well. This scattering and backscattering leads to a widening and distortion of the exposed region and results in a degradation of the resolution of two parallel e-beam lines. It is clear from this study that the ultimate resolution of the e-beam process is determined by electron scattering effects in the resist material and by electron backscattering from the device substrate, and not by the resolution of the electron-optical system. In this paper we assess the merit of the e-beam fabrication technique for use in very high speed integrated circuit (VHSIC) technology. A study is presented which describes the electron scattering and backscattering processes in electronic materials. A theoretical study describing primary electron backscattering from single and double-layered substrates is presented; also attention is focused on the question of the spatial region exposed by a scattered electron beam in a lithographic resist material. Experimental electron backscattering, e-beam and scanning electron microscopy studies are presented to corroborate theoretical predictions.

ELECTRON BACKSCATTERING

Many phenomena, such as polymer bond breaking, x-ray production, cathodoluminescence, electron-hole pair generation in semiconductors and insulators, etc., result from the inelastic interaction of a high energy (1-50 keV) electron beam with matter. Numerous primary electron backscattering studies, both experimental and theoretical, have been carried out in an effort to understand the dominant mechanisms for electron scattering and energy loss arising from the electron beam-target interaction. Most theoretical treatments (1-3) of electron backscattering are limited in usefulness, suffering either from severe physical approximations or mathematical complexity. However, the recent theoretical extension (4) of Everhart's theory (1) to include the calculation of energy distribution spectra has stimulated a renewed interest in this simple analytic approach.

In this paper we make use of Everhart's theory (1,4) to describe electron backscattering from solids, double layers, and supported thin films. [Due to limitations in space, only salient features of the theory will be discussed throughout the paper. Detailed theoretical analyses and discussions can be found in the references cited.] Everhart's theory assumes that primary electrons, upon entering a solid target, suffer energy loss in accordance with the Thomson-Whiddington (T-W) law and undergo changes in direction via single large-angle (greater than 90°) Rutherford scatters. Moreover, electrons that are scattered through angles less than 90° are treated as if they are not scattered at all.

The T-W energy-loss law asserts that the energy loss associated with a typical particle at a given depth into the target is inversely proportional to the energy of the particle at that depth. Thus, in making use of the assumptions of Everhart's theory, the relative number of electrons backscattered from a solid target of atomic number Z with energies in the range $(\varepsilon E_0, E_0)$, where E_0 is the primary electron energy and ε is some fraction of E_0, can be calculated as

$$\eta_s(\varepsilon,Z) = \frac{(a+1)y_0 - 1 + (1-y_0)^{a+1}}{(a+1)y_0} \tag{1}$$

where

$$y_0 = \tfrac{1}{2}(1-\varepsilon^2) \tag{2}$$

and

$$a = (0.045)Z. \tag{3}$$

1. T. Everhart, J. Appl. Phys. 31, 1483(1960).

2. G. Archard, J. Appl. Phys. 32, 1505(1961).

3. R. Dashen, Phys. Rev. 134, A1025(1964).

4. G.J. Iafrate, W.S. McAfee, and A. Ballato, J. Vac. Sci. Technol., 13, 843(1976).

The energy distribution curve (EDC) can be obtained, to within a factor $(1/E_0)$, directly from the absolute value of the first derivative of $\eta_s(\epsilon,Z)$ with respect to ϵ. Figures 1 and 2 show the dependence of $\eta_s(\epsilon,Z)$ and the EDC on ϵ for various values of Z; since ϵ is the reduced energy with which the least energetic electrons in the backscattering current, $\eta_s(\epsilon,Z)$, escape from the target, it is then also thought of as the reduced potential energy required to retard backscattered electrons with reduced energies less than ϵ from being collected by an electron analyzer. Figure 2 indicates two salient features of the EDC as predicted by Everhart's theory, namely, the general "triangular" shape of the curve and the change in curvature of the EDC's from concave downward to concave upward with increased Z.

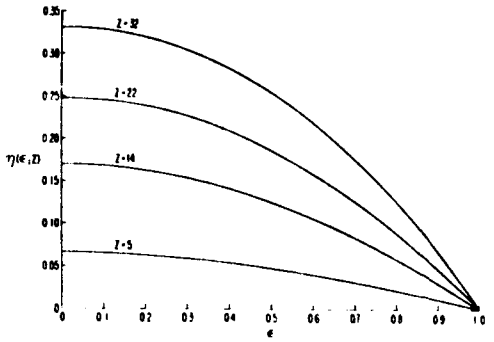

ELECTRON BACKSCATTER COEFFICIENTS FOR B, Si, Ti & Ge FOR VARIOUS RETARDING VOLTAGES

Fig. 1.

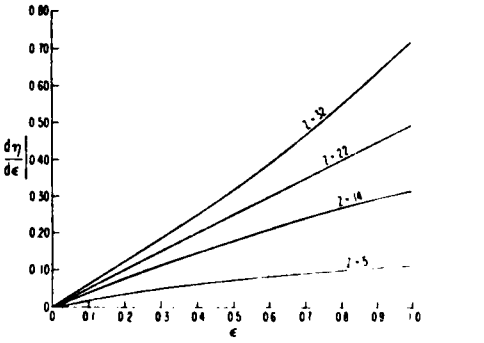

ENERGY DISTRIBUTION CURVES FOR ELECTRONS BACKSCATTERED FROM B, Si, Ti & Ge

Fig. 2.

These two features have been observed in the experiments of Kulenkampff and Spyra (5) as shown in Fig. 3. The poor agreement between theory and experiment for Z = 78 (Pt) in Fig. 3 is expected since diffusion as given by Archard's theory (2), rather than single scattering in accordance with Everhart's theory (1), is believed to be dominant for $Z \gtrsim 40$. In addition, the lack of agreement between theory and experiment for Cu and Al when $\epsilon \lesssim 1$ is believed to be due to the failure of the T-W continuous energy-loss law (indeed, any continuous energy-loss law) near the target surface. (6,7)

5. H. Kulenkampff and W. Spyra, Z. Phys. 137, 416(1954).

6. D. Brown, D. Wittry, and D. Kyser, J. Appl. Phys. 40, 1627(1969).

7. L. Spencer and V. Fano, Phys. Rev. 95, 1172(1954).

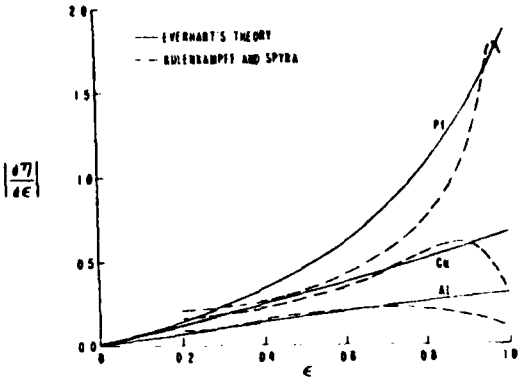

Fig. 3. Comparison of EDC's of Everhart's theory with those experiments obtained in ref. (6) for Al, Cu, and Pt.

We point out in Fig. 1 that the relative number of electrons backscattered from reasonably-high-Z solids such as silicon (Z = 14) and gallium arsenide (Z = 33) can be quite high, ranging from 17% to about 35% respectively. For solids with higher nuclear charge, such as gold (Z = 79), the relative number of backscattered electrons can be as high as 65%.

Finally, we note that the backscattering coefficient derived in this analysis does not depend explicitly on the incident electron energy when the retarding potential energy, ϵ, is zero. This is a result which seems to be consistent with the experimental data reported by Sternglass (8) and others for primary electron energies above 3-5 keV.

Everhart's theory can easily be extended (4) to describe electron backscattering from double layers and supported thin films. In the analysis the target is considered to be a double layer consisting of an infinitely thick substrate covered by an overlying thin film of thickness D. The thin film and substrate are assumed to have mass density and average atomic number (ρ_1, Z_1) and (ρ_2, Z_2), respectively. When the maximum depth of electron penetration is less than or equal to the thin film thickness, D, the electrons energetically can only backscatter from the thin film; the appropriate backscattering coefficient is then given by $\eta_s(\epsilon,Z)$ in Eq. (1) with Z replaced by Z_1. On the other hand, when the maximum depth of electron penetration is greater than D, electrons then have sufficient energy to backscatter from both thin film and substrate. In this case the backscattering coefficient is given by

$$\eta(\epsilon,Z_1,Z_2) = \eta_{TF} + \eta_{TFS} \qquad (4)$$

8. E.J. Sternglass, Phys. Rev. 95, 345(1954); P.C.R. Palluel, C.R. Seances Acad. Sci. Roum. 224, 1492(1947).

Here, η_{TF} represents the reflection coefficient for electrons backscattered from the thin film of thickness D and η_{TFS} is the reflection coefficient for electrons transmitted through the thin film and then backscattered from the substrate with sufficient energy to escape from the target.

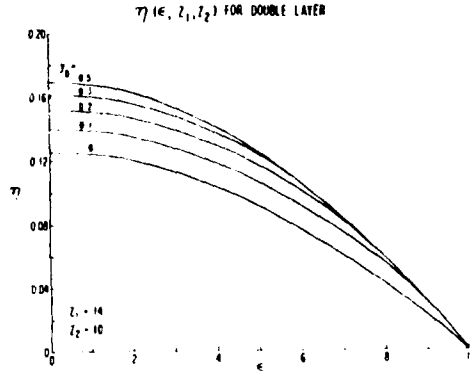

Fig. 4. Backscattering coefficient for double layer targets. Z_1 and Z_2 refer to the average nuclear charge of the thin film and substrates, respectively; y_D is the reduced thin film thickness.

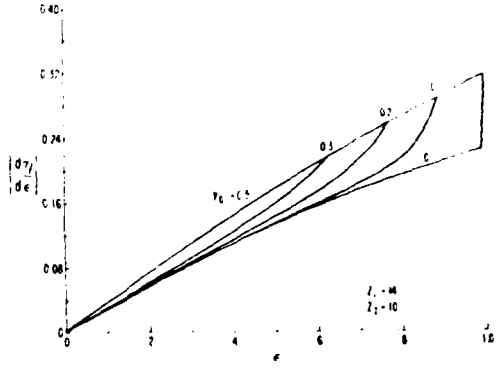

Fig. 5. EDC's for double-layer targets. Z_1 and Z_2 refer to the average nuclear charge of the thin film and substrates, respectively; y_D is the reduced thin film thickness.

The backscattering coefficient and the EDC derived therefrom are plotted as functions of ε in Figures 4 and 5 for $Z_1 = 14$ and $Z_2 = 10$, and for various values of y_D [y_D is the reduced thin film thickness D/R_1, where R_1 is the range of electrons in the thin film]. For $\varepsilon \lesssim \varepsilon_c = (1-2y_D)^{1/2}$, the backscattering coefficient veers away from its "bulk" thin film value to accommodate the composite thin film-substrate scattering. This variation in the backscattering coefficient is greatly enhanced in the EDC's of Fig. 5, and is due to the assumed discontinuous nature of the interface; a sigmoidal variation in Z and ρ across the interface should lead to a smooth variation in the EDC's.

Experimentally measured EDC's for double-layer supported thin film targets appear not to be available in the literature, so that comparison with theory could not be made. There are, however, many experiments for double layers and supported thin films which relate the backscattering coefficient to the thin film mass thickness ρD and primary electron energy E_0. Holliday and Sternglass (9) have reported backscattering coefficients as a function of primary electron energy for various double-layer targets. In Fig. 6 we compare the theoretical backscattering coefficient with their results to show good agreement.

9. J. Holliday and E. Sternglass, J. Appl. Phys. 28, 1189 (1957).

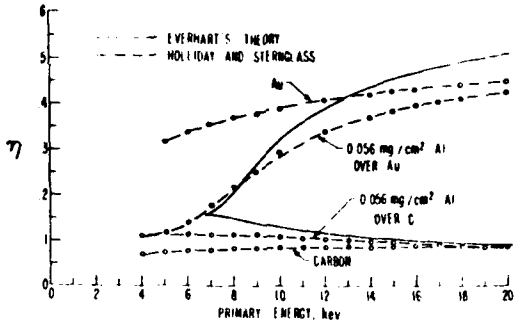

COMPARISON OF η FOR MULTILAYER FILMS OF ALUMINUM OVER GOLD AND ALUMINUM OVER CARBON

Fig. 6.

In addition, Cosslett and Thomas (10) have reported electron backscattering coefficients as a function of mass density and primary electron energy for thin films supported on rings. In Fig. 7 we compare our backscattering coefficient with experimental results to show reasonable agreement.

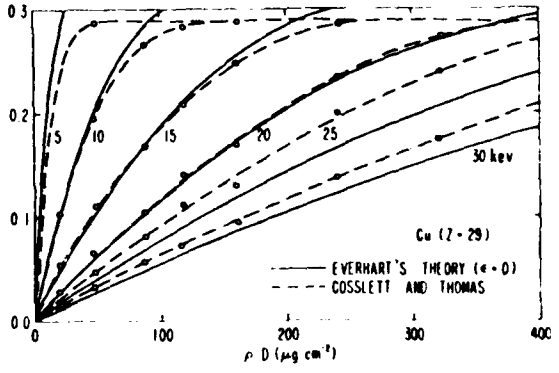

Fig. 7. Comparison of η_{TF} with experiment for Cu.

Comparison of theoretically obtained backscattering coefficients and EDC's with results obtained by experiment yielded good agreement, which is remarkable in view of the simplicity of Everhart's assumptions and the adopted model for the double-layer interface. Moreover, we have pointed out that, within this model for which we have established reasonable confidence, the percentage of incident electrons reflected from a solid or double-layered substrate will increase monotonically with the atomic number of the reflecting substrate. It will be shown in a later section that this behavior affects the resolution of closely spaced e-beam lines rather dramatically.

10. V. Cosslett and R. Thomas, Br. J. Appl. Phys. 16, 779(1965).

ELECTRON SCATTERING

In this section we address the question of the spatial extent of electrons scattered in the target. We do this by making use of the multiple scattering theory of Bethe et al. (11,12) to calculate the average cosine between the actual direction of motion and the direction of the primary beam in terms of the average atomic number of the target and the depth of electron penetration into the target. Moreover, we make use of the order-of-magnitude expression for the depth at which two e-beam lines overlap in terms of the average atomic number of the target.

Bethe et al. (11,12) have established the average cosine between the actual direction of motion and the direction of the primary beam for fast electrons to be

$$\langle\cos\theta\rangle = \exp\left[(-2)\int_{E_d}^{E_0} \frac{dE}{\lambda\left|\frac{dE}{dx}\right|}\right] \tag{5}$$

where λ is the "transport mean free path", $|dE/dx|$ is the energy-loss law for primary electrons moving through the target, E_0 is the incident electron energy, and E_d is the energy of electrons at depth d. It follows from reference (2) that the $\langle\cos\theta\rangle$ can be expressed as

$$\langle\cos\theta\rangle = (1-y_D)^{7Z/40} \tag{6}$$

where the normalized depth y_d is the depth "d" penetrated divided by the range, R, of the electrons in a solid of atomic number Z. In Fig. 8 we plot the $\langle\cos\theta\rangle$ of Eq. (6) as a function of normalized depth, y_d, while treating the atomic number, Z, as a parameter. It is clear from this figure that, as a function of normalized depth, the $\langle\cos\theta\rangle$ tends to zero with increasing rapidity as the target nuclear charge increases. This means that, for a fixed normalized depth of penetration, the electrons will scatter through an "average" angle which increases monotonically with target nuclear charge.

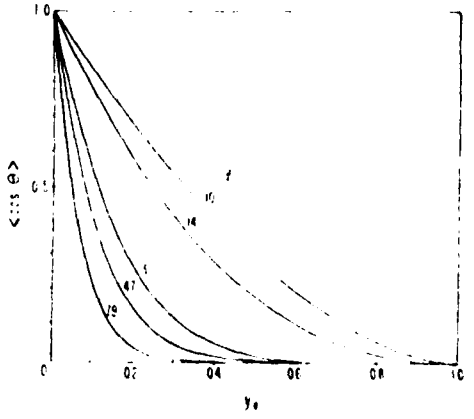

Fig. 8. Plot of $\langle\cos\theta\rangle$ as a function of normalized depth, y_D, with average atomic number, Z, as a parameter.

11. H. Bethe, Rose, and Smith, Proc. American Philosophical Society, 78, 573(1938).

12. H. Bethe, Ann. Physik, 5, 325(1930).

This finding has significant importance in the light of recent work reported by IBM (13) on high atomic-numbered (Z) acrylic polymer resist compositions. IBM has studied Thallium (Z = 81) and cesium (Z = 55) substituted methacrylic acid copolymers which have average atomic numbers (Z) higher than Z-values of well-known resist polymers such as poly(isobutylene)(Z = 2.6), poly(methyl methacrylate)(PMMA) (Z = 3.6), and poly(butene-1-sulfone)(Z = 4.1); the value of Z for 100% cesium-substituted acrylic polymer resist is 11. In a later section electron scattering in the resist will be shown to be a factor governing e-beam pattern resolution.

One can make use of the $\langle\cos\theta\rangle$ calculation to establish the dependence of the undercutting on target nuclear charge of two equally exposed parallel electron-beam lines. We define L, somewhat arbitrarily, as the depth at which electrons scattered from each beam mutually expose the region of the target midway between the two electron-beam lines. The depth L is then determined by setting the $\langle\cos\theta\rangle$ equal to the geometrical cosine, $\cos\theta_g = 1/[1 + 1/4(D/L)^2]^{\frac{1}{2}}$, depicted in Fig. 9. We set the $\langle\cos\theta\rangle$ in Eq. (6) [with d = L] equal to $\cos\theta_g$ to obtain an analytical expression for the normalized depth, $\mathcal{L}$, as

$$(1-\mathcal{L})^{7Z/40} = 1/[1 + 1/4(\mathcal{D}/\mathcal{L})^2]^{\frac{1}{2}} \tag{8a}$$

with

$$\mathcal{D} = D/R, \quad \mathcal{L} = L/R, \tag{8b}$$

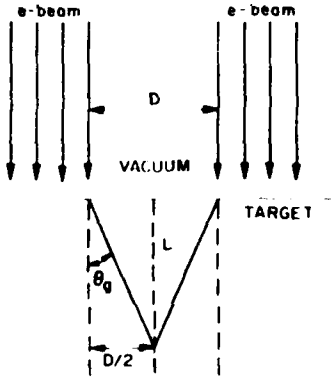

Fig. 9. Diagram depicts two e-beams, separated by a distance D, striking the target; the geometrical angle, θ_g, and the undercutting length, L, are visually defined.

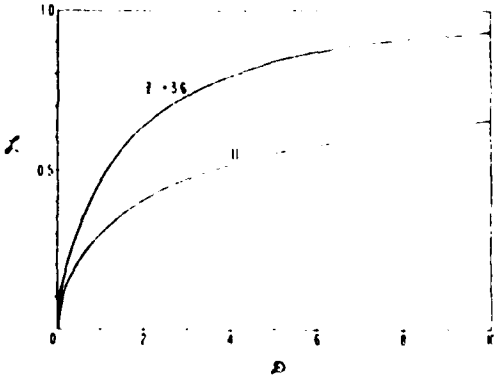

Fig. 10. Plot of reduced depth, $\mathcal{L}$, as a function of reduced separation, $\mathcal{D}$, with average atomic number, Z, as a parameter.

13. R. Feder, T. Haller, M. Hatzakis, L.T. Romankiw, and L. Spiller, IBM Technical Disclosure Bulletin, 18, 2346(1975).

Here, as before, R is the range of the electron in the target material. In Fig. 10 we plot the reduced depth $\mathcal{Z}$ as a function of reduced separation between electron beams with average atomic number as a parameter. The results predict a marked decrease in the depth $\mathcal{Z}$ with increased target nuclear charge for a fixed separation between electron beams. We also note from Fig. 10 that increasing the average atomic number of the resist from 3.0 to 11 radically changes the dependence of undercutting on the spacing of the electron beams.

ELECTRON-BEAM LITHOGRAPHIC STUDIES

In the previous sections of this paper, we have outlined two theoretical models which adequately describe electron backscattering and scattering phenomena in solids. Moreover, we made several observations based on the theoretical results, namely, that a substantial fraction of incident electrons can be reflected from a semiconductor surface or interface and that the spatial extent of penetrating electrons scattered from an incident electron beam is strongly dependent on the average nuclear charge of the target. We now show that both of these phenomena dramatically affect the resolution of closely spaced e-beam lines.

Experimentally, we have studied electron scattering and backscattering effects in "infinitely thick" resist materials and in thin film resist materials mounted on various IC substrates. [The terms "infinitely thick" and "thin" film refer to the thickness of the film relative to the range of the electrons.] In this study we have irradiated a variety of substrates by EBL techniques; the resulting e-beam exposures were then photographed by use of scanning electron microscopy (SEM). In our EBL process a 20 keV electron beam exposes a radiation-sensitive target [PMMA was used in this study] overlaid on an IC substrate; a subsequent chemical development treatment removes the exposed region leaving an outline of the pattern created by the scattered electron beam. Figure 11 represents an SEM photograph of a

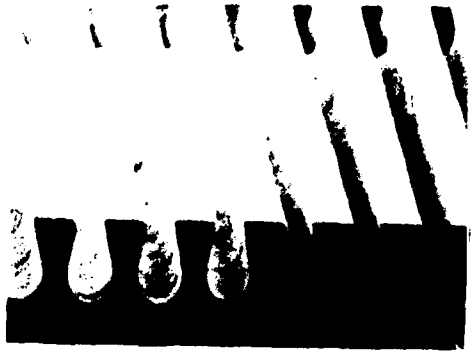

Fig. 11. SEM photograph of a typical EBL exposure of thick PMMA resist material.

typical EBL exposure of thick PMMA resist material. For this particular pattern, the e-beam machine was programmed to "write" ten equally-spaced one-micron-thick lines of two-micron spacings. The teardrop-shaped hollows represent developed regions of e-beam exposure. The geometrical shape of a given hollow is directly related to the spatial extent of the scattered e-beam in the resist material. It is clear from this figure that e-beam scattering in the resist will limit the e-beam line separation achievable in EBL; as the e-beam line separation is reduced, the teardrops below the surface overlap to undercut the resist material between the lines, thereby destroying the e-beam pattern.

In order to study the depth of undercutting as a function of e-beam separation in PMMA without destroying the e-beam pattern, we have developed a unique technique which makes use of the misalignment of the e-beam deflection fields. The deflection field is the maximum area of e-beam projection achievable without translating the e-beam specimen stage. Since the e-beam machine in our laboratory writes with a deflection field of 0.5 x 0.5 square millimeters, to write larger patterns covering areas greater than the deflection field requires precise matching (butting) of the adjacent deflection fields. If adjacent deflection fields are not well matched, then an e-beam pattern which is written across the deflection field boundary will give rise to a "butting" error. The e-beam pattern resulting from a lateral (transverse) adjacent deflection field mismatch is seen in Fig. 13c. In our study we intentionally misalign the adjacent deflection fields in the longitudinal direction with respect to ten equally spaced e-beam lines. In this case the e-beam lines in the array are doubly exposed at the deflection field boundary. Thus, when the pattern is developed, the doubly exposed regions at the field boundaries produce much deeper crevasses whose internal shapes resemble the e-beam patterns receiving twice the dose. For our purposes, we write the entire pattern with an underexposing e-beam dose; since the field boundary receives double exposure, the PMMA samples fracture very easily at the field boundary thus making visable the e-beam radiation pattern without destroying the pattern. An SEM photograph of a typical sample is seen in Fig. 12. In this figure it should be noted that a triangular region is defined between the underexposed e-beam lines as theoretically visualized in Fig. 9. We have written a series of arrays, varying the spacings between one-micron-thick lines, while keeping the e-beam exposure rate and misaligned deflection field constant, to obtain the depth of undercutting as a function of line spacing. The results indicate excellent agreement with the shape of the curve predicted in Fig. 10 for PMMA ($Z = 3.6$).

Fig. 12. SEM photograph of e-beam radiation pattern.

Finally, we have experimentally studied e-beam proximity effects [overexposure effects arising from e-beam writing of closely-spaced lines and from electron backscattering from substrates] on thin films of PMMA due to substrate electron backscattering. We have already established in a previous section that the percentage of incident electrons backscattering from a substrate will increase with the atomic number of that substrate. We have e-beam irradiated three different samples to show dramatic proximity effects.

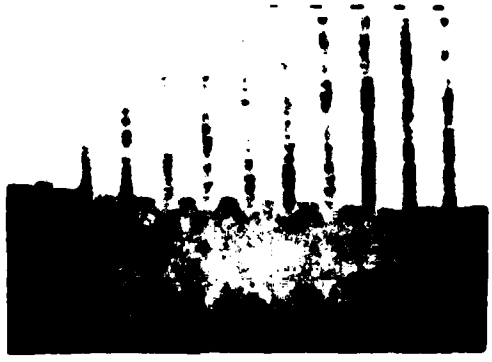

Fig. 13a. SEM photograph of e-beam exposure on PMMA.

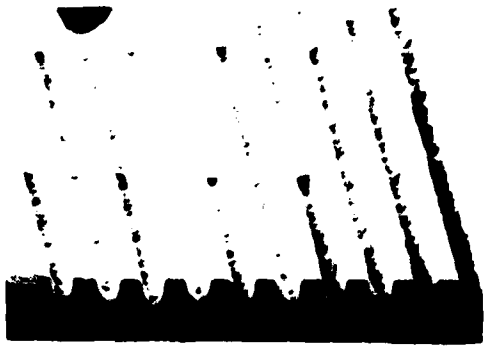

Fig. 13b. SEM photograph of e-beam exposure on PMMA/silicon substrate.

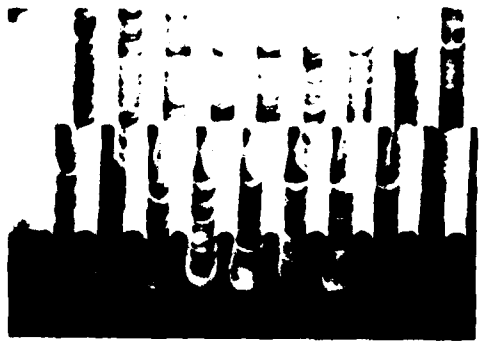

Fig. 13c. SEM photograph of e-beam exposure on PMMA/gold substrate.

In Figure 13a we show an e-beam exposure on "infinitely thick" PMMA. In Figures 13b and 13c, we show typical e-beam exposures of three-microns-thick PMMA on silicon (Z = 14) and gold (Z = 79), respectively. All three samples were exposed to equal e-beam doses, yet the samples show an increased e-beam over-exposure with increased substrate nuclear charge. Thus, we have clearly shown that e-beam scattering effects play a major role in limiting the resolution of closely spaced e-beam lines.

SUMMARY

In this paper two theoretical models have been outlined which adequately describe electron backscattering and scattering phenomena in solids. The theoretical results indicated that a substantial fraction of incident electrons can be backscattered from a semiconductor substrate and that the spatial extent of penetrating electrons from an incident electron beam is strongly dependent on the average nuclear charge of the target. Experimentally, we have shown that both of these phenomena dramatically affect the resolution of closely spaced e-beam lines. As part of our experimental study, we have developed a technique for studying closely-spaced e-beam patterns without destroying the pattern.

In future studies we plan to expand our theoretical efforts to include the simulation of e-beam patterns by using a further extension of Everhart's theory as well as Monte Carlo methods. Experimentally, we plan to extend our present studies to include a wide variety of resist materials and substrates by using the excellent EBL and SEM facilities available in ET&DL.

ACKNOWLEDGMENTS

The authors wish to thank D. Eckart for technical assistance.


DATE
ILMED
-8